

# INDEPENDENT CALIBRATION OF RADAR REFLECTIVITIES USING RADIOSONDES : APPLICATION TO ESRAD

Sheila Kirkwood<sup>1</sup>, Maria Mihalikova<sup>1</sup>, Daria Mikhaylova<sup>1</sup>, Ingemar Wolf<sup>1</sup>, and Phillip Chilson<sup>2</sup>

<sup>1</sup>*Polar Atmospheric Research, Swedish Institute of Space Physics, Box 812, 98128 Kiruna, Sweden,  
sheila.kirkwood@irf.se, maria.mihalikova@irf.se, daria.mikhaylova@irf.se, ingemar.wolf@irf.se*

<sup>2</sup>*School of Meteorology and Atmospheric Radar Research Center, University of Oklahoma, 120 David L. Boren Blvd.,  
Rm 4618, Norman, OK 73072-7307, USA, chilson@ou.edu*

## ABSTRACT

A large number of empirical and theoretical studies have shown that radar reflectivity from the atmosphere at 50 MHz is proportional to the mean vertical gradient of the refractive index. Up to 30 km height the refractive index is determined by temperature, pressure and humidity profiles, which can readily be measured by radiosondes. In practice, humidity becomes unimportant above the mid-troposphere. The coefficient of proportionality between radar reflectivity and mean refractive index gradient should, in principle, depend on the fine-scale structure of refractive index fluctuations. However, recent empirical evidence shows that the coefficient varies very little between widely different meteorological conditions and between radars in very different locations (Esrang, tropical India, Antarctica). This means we can use mean profiles of refractive index, measured by radiosondes, as an independent method to provide continuous calibration of radar reflectivity and to cross-calibrate between different radars without the need to interrupt operations for the kind of engineering tests which are usually used for calibration. We show how this can be applied for long-term calibration of the 52 MHz atmospheric radar at Esrange, ESRAD.

The observed invariability of the coefficient of proportionality also poses an intriguing question as to how it can be explained. High-resolution sondes, constant-height sondes, and UAV's are suggested as suitable platforms for further study of the radar scattering mechanisms.

Key words: L<sup>A</sup>T<sub>E</sub>X; ESA; macros.

## 1. INTRODUCTION

VHF atmospheric radars are widely used in the study of radar echoes from the mesosphere, such as Polar Mesosphere Summer and Winter Echoes (PMSE and PMWE). The mechanisms behind these radar echoes are not yet completely understood and a number of campaigns using

sounding rockets to measure fine-scale structure in-situ have been carried out. In order to test the various theories relating the fine-scale structure to the strength of the radar echoes, it is important to be able to express that strength in absolute physical units. There is the same need when radar measurements are compared between different sites and different radars, and with satellite-based or other ground-based observations of related phenomena such as noctilucent clouds. Absolute values of the scattering cross-section are also of interest in testing theories of scattering from the lower atmosphere, for example in the upper troposphere and lower stratosphere, where scatter is highly aspect sensitive (i.e. much stronger close to zenith).

Scatter from mesospheric echoes is usually assumed to be due to isotropic scatterers in which case the parameter 'volume reflectivity' is the appropriate measure of scattering cross-section. For highly aspect-sensitive echoes the parameter 'Fresnel scatter' is more appropriate. Values of volume scatter ( $\eta$ ) or Fresnel scatter ( $\frac{|\rho|^2}{\Delta r}$ ) can be calculated from radar observations as follows [1, 2]:

$$\frac{|\rho|^2}{\Delta r} = \frac{P_r}{P_t} \frac{4\lambda^2 r^2}{L_t A_{eff}^2 \Delta r} \quad (1)$$

$$\eta = \frac{P_r}{P_t} \frac{64(2\ln 2)r^2}{\pi L_t V_f A_{eff} \Delta r} \quad (2)$$

where  $P_t$  is power delivered to the antenna,  $P_r$  is power due to atmospheric scatter received by the antenna,  $r$  is the distance to the scattering volume,  $\Delta r$  is the thickness of the volume element along the radar beam,  $\lambda$  is the radar wavelength,  $A_{eff}$  is the effective area of the receiving antenna,  $L_t$  accounts for losses in the antenna feed on transmission ( $<1$ ) and  $V_f$  expresses the fraction of the scattering volume which is filled with scatterers ( $\leq 1$ ).

Estimates of the absolute values of these parameters require that the transmitted power, the losses in the antenna, and the antenna gain ( $G = 4\pi A_{eff}/\lambda^2$ ) are known. In

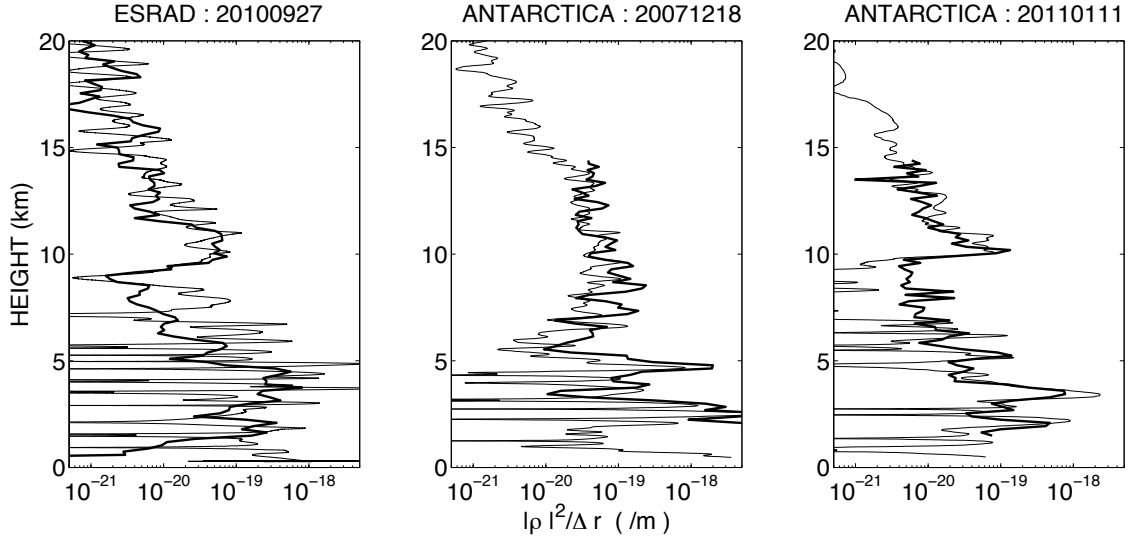


Figure 1. Examples of profiles of Fresnel scatter measured using the ESRAD radar in the Arctic and the MARA radar in Antarctica, using Eq. 1 and engineering measurements of radar calibration parameters (thick lines) and calculated as  $2 \times 10^{-3} M^2$  from high-resolution radiosonde measurements (thin lines). The radiosondes were launched from the radar sites.

addition, the receivers must be calibrated, and the data-processing known, so that the final digital output of the (coherently) integrated and time-averaged signal can be expressed in terms of watts arriving at the receiver pre-amplifiers. We can write  $P_r = \gamma S$ , where  $S$  is the signal power, in some unknown units, after the signal processing, and  $\gamma$  is the conversion factor to physical units, which needs to be found by calibration. Although it is in principle possible to measure all the necessary parameters by engineering tests, this is usually done only occasionally, which leaves much room for uncertainty between tests. For example, signal or noise injection may be used to calibrate the receivers. Continuous monitoring of the daily variation of galactic noise (essentially a noise injection source calibrated by radio-astronomers) allows continuous calibration of the receivers [see e.g. 5], but this still leaves the problem of other parameters which may vary over time (such as transmitter power and antenna loss). There is also much scope for human error in applying the results of engineering tests to the final result of the data processing. Fortunately a better solution is available.

## 2. UTLS FRESNEL SCATTER

The theory of Fresnel scatter from the non-ionised atmosphere predicts that [1]:

$$\frac{|\rho|^2}{\Delta r} = F^2(\lambda) M^2 \quad (3)$$

where  $F(\lambda)$  is a measure of the fine structure of refractive index variations in the vertical direction at half the

radar wavelength and  $M$  is the mean vertical gradient of generalised potential refractive index :

$$M = -77.6 \times 10^{-6} \frac{p}{T} \frac{\delta \ln \theta}{\delta z} \left[ 1 + \frac{15,500q}{T} \left( 1 - \frac{1}{2} \frac{\delta \ln q / \delta z}{\delta \ln \theta / \delta z} \right) \right] \quad (4)$$

where  $p$  is pressure in hPa,  $\theta$  is potential temperature,  $T$  temperature, both in K and  $q$  is the specific humidity in  $\text{kg kg}^{-1}$ . This means that, in the troposphere and lower stratosphere,  $M$  can be determined from radiosondes. It has also been found that, for the upper troposphere and lower stratosphere (UTLS) the value of  $F$  does not vary significantly over time (averages over 10s of minutes, time periods of several days) or height [e.g. 3, 4]. Indeed, it has been found that  $F$  does not vary significantly even between locations with very different meteorology [Arctic Sweden, tropical India and Antarctica, 5]. The value found for the 50 - 55 MHz radars in the latter study was  $F^2 = 2 \times 10^{-3}$ .

Fig. 1 shows examples of the comparison between Fresnel scatter measured by the ESRAD 52 MHz radar at Esrange (Arctic Sweden) and that calculated predicted from radiosonde measurements. The ESRAD measurements, which have 150m vertical resolution, use calibration by galactic noise, measured antenna loss, nominal transmitter power and simulated effective area). For the radiosondes, Fresnel scatter is calculated as  $F^2 = 2 \times 10^{-3}$ , where  $M$  is calculated from the temperature, pressure and humidity profiles measured by the sondes. All of the sondes were launched from Esrange.

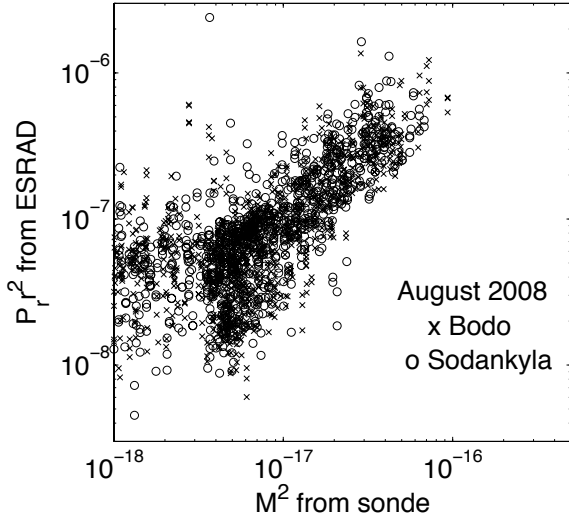


Figure 2. Scatter plot of  $P_r r^2$  from ESRAD as a function of  $M^2$  from radiosondes for a typical month - August 2008. Measurements between 8 and 16 km heights are used.  $M^2$  values are calculated using measurements from Bodo and Sodankyla from the archive of standard radiosonde results at University of Wyoming.

### 3. RADAR CALIBRATION BY RADIOSONDES

Since all empirical evidence points to constancy of the value of  $F$  in Eq. 3 (for the UTLS region), we can use radiosondes as an independent calibration for any 50 - 55 MHz radar. Specifically, if we want to determine the radar scatter cross-section at a height  $z$  and are measuring radar profiles covering UTLS heights as well, and processing the digitised samples from all heights in the same way, we can replace Eqs. 1 and 2 with :

$$\frac{|\rho|^2}{\Delta r} = X_s F^2(\lambda) S_z r_z^2 \quad (5)$$

$$\eta = Y_s F^2(\lambda) S_z r_z^2 \quad (6)$$

where

$$X_s = \langle \frac{M^2}{S_r^2} \rangle_{UTLS} \quad (7)$$

and

$$Y_s = \frac{16(2 \ln 2) A_{eff} X_s}{\pi \lambda^2} \quad (8)$$

where  $S$  is the signal power in arbitrary units, after data processing,  $M^2$  are values determined from radiosondes and  $\langle \rangle_{UTLS}$  represents the average value of the ratio between corresponding values from the radiosondes and the radar in the UTLS region. In other words, we no longer

need to monitor the transmitted power, the antenna losses or the conversion factor from digital output to watts. We need only to compare with radiosondes in the UTLS, and apply a constant factor (multiplied also by the antenna gain in the case we want to consider volume scatter). We can also apply Eqs. 5 and 6 to times when no radiosondes are available, if we are confident that no changes in radar characteristics, operating parameters or signal processing have occurred since a radiosonde calibration was possible.

In the (usual) case where the receiver response and the signal processing details are recorded continuously, we can calculate  $X$  using  $P_r$  instead of  $S$ . In this case, we can further use variations in the value of  $X$  over time as a diagnostic of radar performance, as  $X$  will be sensitive to changes in transmitter power and antenna losses.

### 4. RESULTS FROM ESRAD

We illustrate the calibration / radar performance monitoring by results from the ESRAD radar, at Esrang, Kiruna, covering the summer months (May-August) in the 13 years from 1997 to 2009. ESRAD is most of the time not heavily affected by disturbing radio transmissions. This allows the receiver response to be monitored by comparing the daily variation in the noise background with the expected daily variation in galactic noise. Also, all raw data has been stored since routine operations began in 1997 so the signal processing details are easy to trace. This means we can readily calculate  $P_r$  instead of  $S$ . Here we use results from a radar mode which uses a 8-bit, 600 m baud, complementary code to measure profiles from 5 km to 100 km height. This radar mode has been in use during the whole 13 years, with only one change of data processing (decreased number of coherent integrations in 2005) during that time.

Radiosondes are not launched regularly at Esrang, only during campaigns. The nearest regular sondes (4 times per day) are launched at Bodo in Norway and at Sodankyla in Finland. These are available from a database at University of Wyoming. The resolution of the profiles in the database is 100 - 500 m, which is much less than for the sondes in Fig. 1, and the horizontal distance between the sonde measurements and the radar can be very large (several 100 km). So we do not expect as close agreement as in Fig. 1. But, we can expect that the sondes, at least some of the time, sample the same synoptic air-masses as the radar and by averaging over a large number of sonde-radar comparisons we can hope to get a reasonable calibration. We average  $M^2$  from the sondes to the same height gates as the radar measurements, and find the average value of  $M^2/P_r r^2$  over the height interval 8 - 16 km for each sonde, using radar data averaged between 0.5 and 1.5 hours after the sonde launch. Fig. 2 shows typical values of  $P_r R^2$  from the radar and  $M^2$  from the sondes, covering a month of observations.

In order to be sure the radar and the sondes are sampling

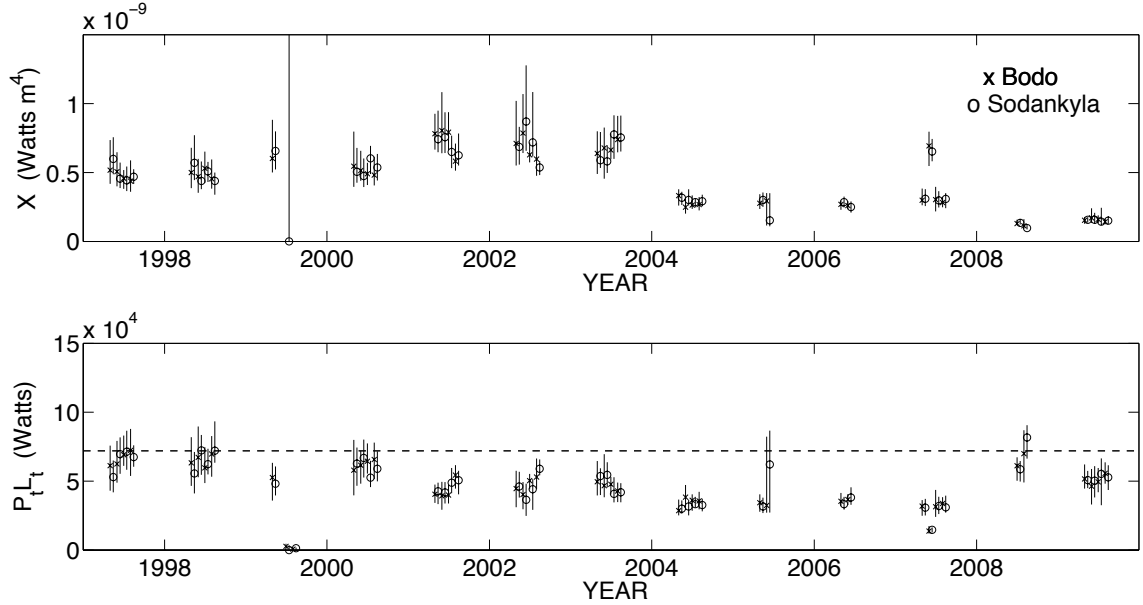


Figure 3. Month-by-month averages of the quantity  $X_p = \langle \frac{M^2}{P_r R^2} \rangle_{UTLS}$  (upper panel) and  $P_t L_t$  (lower panel) for the ESRAD radar, for summer months May-August, years 1997-2009. Measurements between 8 and 16 km heights are used, with 600 m height resolution.  $P_t L_t$  is derived from the  $X$  values  $i$  by correcting for known radar characteristics, including a doubling of antenna effective area from 2004, and assuming  $F^2(\lambda) = 2 \times 10^{-3}$ . The dashed line shows the ideal value - 72 kW.

the same synoptic air masses, we include results only when there is a reasonable correlation between height profiles of  $P_r R^2$  from the radar and  $M^2$  from the radiosondes (correlation coefficient  $>0.7$ ). We also use only times/heights when  $M^2 > 5 \times 10^{-18}$  as the ESRAD measurements become very uncertain below this limit. We then compute mean values of  $X_p = \langle \frac{M^2}{P_r R^2} \rangle$  for each month. The results are shown in Fig. 3 (upper panel). It is clear that the values obtained by comparing to sondes from Sodankyla are close to those for the sondes from Bodo. There is mostly good consistency between consecutive months in the same summer season. The large step in values is due to a change in the antenna size in 2004 (the antenna area was doubled). Other changes are due to deteriorating radar performance during some periods, with recovery after maintenance work. This is better illustrated by the lower panel in 3 where we correct for changes in  $A_{eff}$  and other known factors and use  $F^2 = 2 \times 10^{-3}$ , to estimate the most variable factor,  $P_t L_t$ . Combining Eqs. 1, 3 and 5 we find :

$$P_t L_t = \frac{4 \times \lambda^2 X_p}{F^2 A_{eff}^2 \Delta r} \quad (9)$$

If we assume that the radar peak power,  $P_t$  has remained roughly constant, Fig. 4 can be interpreted as showing changes in antenna loss  $L_t$ . Low values in 1999 are due to known problems following lightning damage. A re-

duction in 2004 coincides with the doubling of area of the antenna array, with longer cables and more complex combiners, introducing higher losses. The stepwise improvement 2008 follows major maintenance work. Fig. 4 shows the same parameters as Fig. 3, but using a radar mode with higher resolution (an uncoded 150 m pulse) and covering all months of the year since mid-2005. The improvement in performance following maintenance in summer 2008 is even clearer here. The low values in October 2009 were due to deliberate operation with low transmitter power and only a small part of the antenna array.

It can also be noted that the values of  $P_t L_t$  are in very reasonable relation to the ideal value (dashed line, corresponding to full nominal transmitter power of 72 kW and no losses in the antenna feed). This tells us that the assumption of a constant value for  $F^2 = 2 \times 10^{-3}$  is more or less correct, winter and summer, and throughout the period covered by this long dataset.

## 5. CONCLUSIONS

We have demonstrated a method for independent calibration of radar scattering cross-section for 50 MHz radar. This can in principle be used to calculate absolute values of Fresnel reflectivity, from height profiles of radar echo power, without any information on the radar characteris-

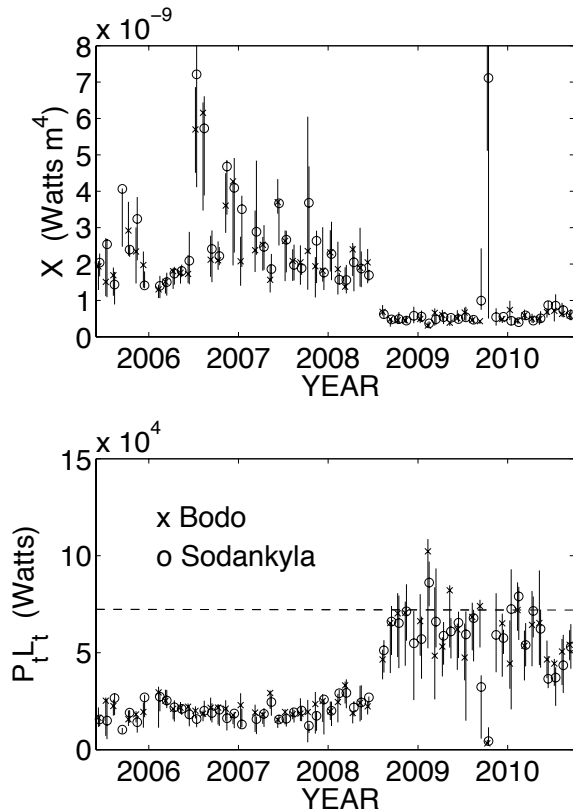


Figure 4. The same parameters as Figure 3, but using measurements with 150 m height resolution, covering all months of the year, from May 2005 to September 2010.

tics or the data processing used. The only requirement is that the height profiles include UTLS heights, and that radiosonde measurements in the same synoptic air masses are available. If the effective antenna area is known, volume reflectivity can also be calculated. (For example, this method has been used to study the variation of PMSE volume reflectivity and its relation of magnetic disturbance levels, at ESRAD, over a 13 year period, in [6].)

In the case that several of the radar characteristics, and the data-processing details are known, the method can instead be used to determine the remaining unknown characteristics. This is demonstrated for ESRAD, where receiver response, antenna sizes and data-processing details are well known. The results show the variation in the product of antenna peak power and transmission loss over the lifetime of the radar so far.

The method is based on an empirical finding [5] that the value of  $F^2$  in Eq. 3 does not vary significantly over time or height, or between widely different locations. There is up to now no physical explanation of this empirical finding. Detailed in-situ measurements of the fine-scale atmospheric structuring responsible for radar echoes will be needed to establish the physical explanation and to

confirm the limits of its variability.

## 6. ACKNOWLEDGEMENTS

ESRAD is operated and maintained jointly by Swedish Institute of Space Physics, Kiruna, and Swedish Space Corporation, Esrange. Standard radiosonde measurements from the the whole globe are archived by University of Wyoming at <http://weather.uwyo.edu/upperair/sounding.html>. Measurements in Antarctica were supported by Swedish Polar Research Secretariat (SWEDARP 2010) and the Finnish Antarctic Program. This project has also been funded by Swedish Research Council Grants 621-2007-4812 and 621-2010-3218.

## REFERENCES

- [1] K. S. Gage, W. L. Ecklund, and B. B. Balsley. A modified Fresnel scattering model for the parameterization of Fresnel returns. *Radio Sci.*, 20:1493–1501, December 1985.
- [2] K.S. Gage. Radar observations of the free atmosphere : structure and dynamics. In D. Atlas, editor, *Radar in Meteorology*, chapter 28a, pages 534–565. American Meteorological Society, Boston., 1990.
- [3] D.A. Hooper, J. Arvelius, and K. Stebel. Retrieval of atmospheric static stability from mst radar return signal power. *Ann. Geophys.*, 22:3781–3788, 2004.
- [4] S. Kirkwood, M. Mihalikova, T. N. Rao, and K. Satheesan. Turbulence associated with mountain waves over Northern Scandinavia - a case study using the ESRAD VHF radar and the WRF mesoscale model. *Atmos. Chem. Phys.*, 10:3583–3599, 2010.
- [5] S. Kirkwood, E. Belova, K. Satheesan, T. Narayana Rao, T. Rajendra Prasad, and S. Satheesh Kumar. Fresnel scatter revisited – comparison of 50 MHz radar and radiosondes in the arctic, the tropics and antarctica. *Annales Geophysicae*, 28(10):1993–2005, 2010.
- [6] M. Smirnova, E. Belova, S. Kirkwood. Polar mesosphere summer echo strength in relation to solar variability and geomagnetic activity during 1997–2009. *Annales Geophysicae*, 29:563–572, 2011.